

# Fully-Automatic Determination of the Arterial Input Function for Dynamic Contrast-Enhanced Pulmonary MR Imaging

Peter Kohlmann, Hendrik Laue,  
Stefan Krass, Heinz-Otto Peitgen  
peter.kohlmann@mevis.fraunhofer.de

Fraunhofer MEVIS  
Institute for Medical Image Computing  
Bremen, Germany

---

## Abstract

Recent studies have shown that dynamic contrast-enhanced pulmonary MR imaging (DCE-pMRI) is a very appropriate imaging technique for the clinical assessment of lung diseases. For the quantitative analysis of pulmonary blood flow (PBF), pulmonary blood volume (PBV), and mean transit time (MTT) an arterial input function (AIF) of the contrast agent entering the lung is required. The AIF is usually calculated from a user-drawn region-of-interest (ROI) within the feeding artery. Thus, the results of the quantitative analysis highly depend on the exact location and the size of the ROI and the reproducibility of the analysis is limited. This work presents a fully-automatic method to determine the AIF within the branching of the pulmonary trunk into left and right pulmonary artery.

## 1 Introduction

Pulmonary perfusion, the blood flow of the lung at capillary level, is closely related to the blood supply of the lung and thus lung function in general. Perfusion is an important functional parameter for the diagnosis of lung diseases. While scintigraphic assessment of perfusion is still the standard clinical tool, MRI is more often used in clinical research settings due to its potential to provide higher resolution and morphologic information. There, intravenous contrast agent (CA) is injected into a patient's blood circulation. To track the progression of the CA through the pulmonary arteries, lung parenchyma, and pulmonary veins, a series of 3D thoracic scans is acquired at short time intervals [4]. Provided that an arterial input function is given, such a data set is sufficient to extract quantitative perfusion parameters (PBF, PBV, and MTT) which are important for diagnosis and therapy planning/monitoring. The basic algorithms to derive these parameters were introduced by Østergaard *et al.* [5] for cerebral perfusion and adapted for pulmonary perfusion, e.g. by Ohno *et al.* [3].

Our clinical partners dealing with lung tumor perfusion and lung perfusion of patients with asthma and chronic obstructive pulmonary diseases (COPD) currently define the AIF by manual drawing of a ROI within the pulmonary artery. An automation of the AIF definition is appreciated due to several aspects. First, it allows the precalculation of perfusion parameter maps already during the import of patient data into the diagnostic reading application. Second, such a technique has the potential to improve the reproducibility of the calculations and to allow the comparability of baseline and follow-up examinations.

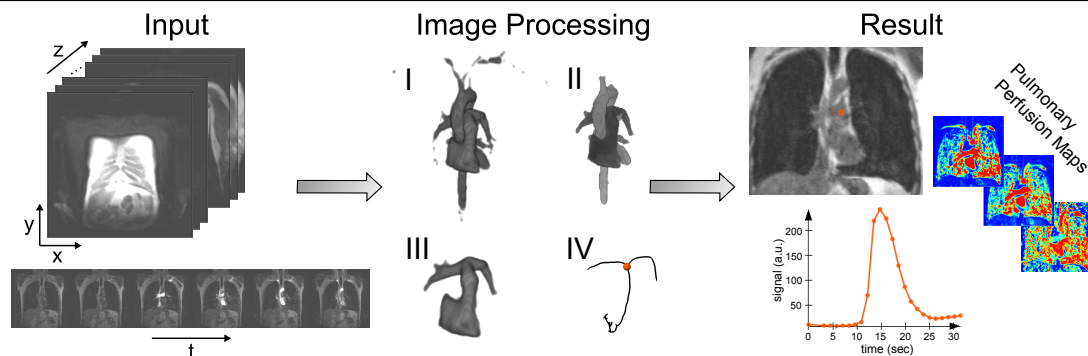


Figure 1: On the input data (left), several successive image processing steps are applied (middle) to automatically determine the AIF and to calculate quantitative perfusion parameter maps (right).

In cerebral perfusion the arterial blood supply is more heterogeneously distributed compared to the lung. Because of the resulting significant effort for the AIF definition, methods for the automatic selection of the AIF were introduced, e.g. by Mouridsen *et al.* [2]. They use k-means clustering to identify automatically the AIF and found out in their evaluation that their method excellently relates to the selections of experienced operators.

Because the blood supply of the lung is controlled by the pulmonary artery we assume that an automatically defined region at a well-defined position within the pulmonary artery is a feasible way to derive the AIF for quantitative pulmonary perfusion analysis. Our method is composed of various successively performed image-processing techniques which are described in this paper. We demonstrate the robustness of the method for a pool of patients suffering from lung diseases. It is subject to future work to compare the method with clustering techniques and to perform a clinical evaluation.

## 2 Material and Methods

First, the properties of the MR data sets are described. Following, the incorporated image processing algorithms of our method are presented. An overview of the results of the individual steps of the presented method is shown in Figure 1. From a 4D MR data set, the position within the pulmonary artery where the pulmonary trunk is branching into left and right pulmonary artery is detected. This position is used to define the AIF which is a required input to calculate quantitative perfusion parameter maps.

### 2.1 Input Data Sets

In DCE-pMRI the image acquisition is performed during and after the intravenous injection of a paramagnetic contrast agent. An appropriate MR sequence is FLASH (fast low-angle shot), which is a T1-weighted gradient echo technique with short repetition time (TR) and short echo time (TE). The typical voxel size of a 3D volume is about  $2 \times 2 \times 5 \text{ mm}^3$  and an appropriate temporal resolution is about 1.3 seconds. To cover the whole thorax and the first pass of the CA, the size of most of our data sets are  $256 \times 256 \times 44 \times 24$  (in x-, y-, z-, t-dimension) voxels. Typically, the patients are instructed to hold their breath during image acquisition. For an excellent introduction of a suggested standard protocol for MRI of the lung the interested reader is referred to an article of Biederer [1].

## 2.2 Image Processing Pipeline

**Removal of unlikely voxels (I):** A data set as described above consists of about 70 million voxels. The vast majority of these voxels can be excluded in a first processing step. For noise suppression a 2D median filter is applied for each slice with a kernel size of 3x3 voxels. Successively, all voxels are excluded which have a very low (background noise) or a very high (fat tissue) initial signal. Following, a temporal maximum intensity projection (tMIP) is calculated, which projects the maximum values along the temporal axis to a 3D volume. All voxels with a signal value less than 25% of the maximum value of the tMIP are excluded from further processing. If the data acquisition was performed properly, the CA flows through the pulmonary artery at its first pass neither within the couple of first nor within the couple of last time steps. Thus all voxels where a rather early or rather late peak in the signal (time-to-peak) is discovered are excluded. Finally, the signal enhancement is analyzed. The peak signal is divided by the baseline signal which is the signal before the CA arrives. In the presented method, the mean signal of the first three time steps serves as baseline signal. All voxels with a peak signal to baseline signal ratio less than four, are excluded. After the application of these steps, the remaining part of an exemplary data set is shown in Figure 1 (Image Processing, I).

**First refinement step (II):** In the first refinement step the goal is to narrow down the remaining voxels to the aorta and the pulmonary artery with the connected chambers of the heart as shown in Figure 1 (Image Processing, II). To remove noise and parts of smaller blood vessels, first a 2D median filter with a kernel size of 5x5 voxels is applied to the remaining voxels from step I. Successively, a 2D morphologic erosion operation is applied with a kernel size of 3x3 voxels. Following, a connected components analysis filters out smaller connected regions and outputs the largest remaining bunch of connected voxels. The last step of the first refinement is the application of a 2D morphologic closing operation with a kernel size of 3x3 voxels to fill holes.

**Second refinement step (III):** The second refinement is performed to remove the aorta and left ventricle. It leaves the pulmonary artery and in most cases the right ventricle as shown in Figure 1 (Image Processing, III). A good way to separate the pulmonary artery from the aorta is a histogram analysis of the time-to-peak data. In the histogram, the pulmonary artery/right ventricle can be clearly separated from the aorta/left ventricle because of a significantly lower time-to-peak. In a thresholding step, the upper threshold is set to the minimum of the valley between the two histogram peaks which correspond to the anatomical features pulmonary artery/right ventricle and the aorta/left ventricle. A successive connected components analysis step results in a segmentation mask including pulmonary artery and right ventricle voxels. This mask is applied to the tMIP image to prepare the image for the image processing step IV, and again 2D median filtering (kernel size: 3x3 voxels) and a closing operation is performed.

**Skeletonization and graph analysis (IV):** A skeletonization step which is based on successive erosion of border voxels is performed on the generated image. The resulting skeleton is shown in Figure 1 (Image Processing, IV). The remaining task is to identify the branching of the pulmonary trunk into the left and right pulmonary artery (illustrated by orange sphere). This is achieved by a graph analysis algorithm which first searches for nodes with exactly

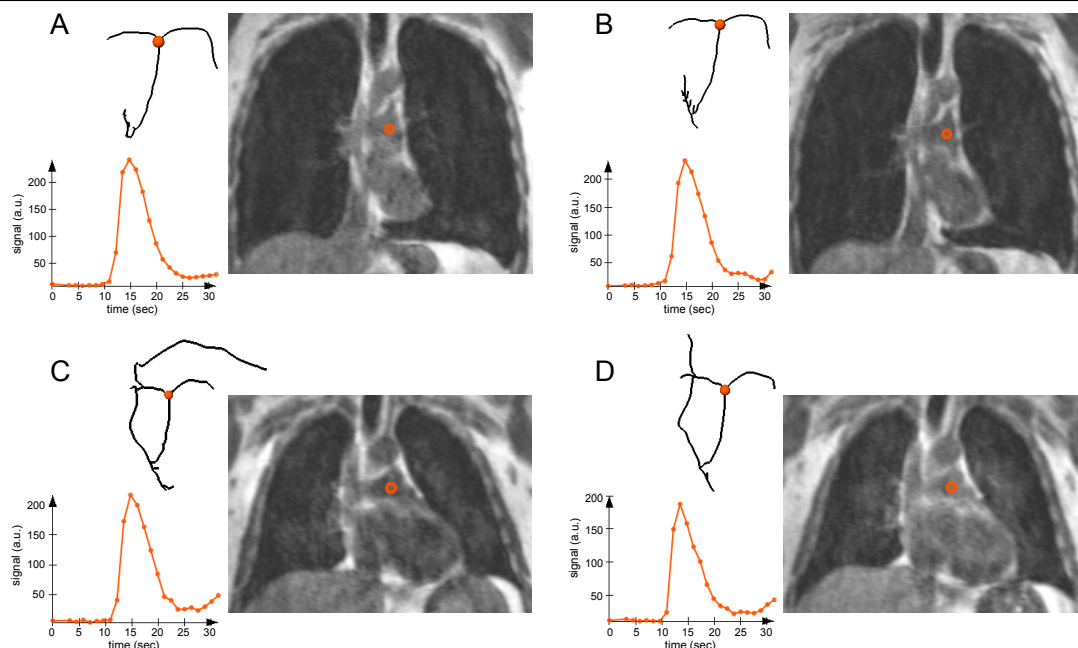


Figure 2: The results of the presented method for baseline examinations (A,C) and the corresponding follow-up examinations (B,D) of two patients.

three edges. If more than one of them exists, a heuristic approach analyzes the spatial node positions, the combined lengths of the edges, and the angles between the edges. Appropriate angles which characterize the sought-after branching points were derived from segmentation masks of the pulmonary artery from a pool of thoracic data sets.

### 2.3 AIF Definition and Parameter Map Calculation

The position which is detected by the described image processing steps is then used to define the AIF. In the current implementation, a circular region around this position which includes 32 voxels (ca.  $610 \text{ mm}^3$ ) is taken into account. The AIF consists of the mean values of these voxels in every time step. The corresponding AIF curve is shown in Figure 1 (Results). Having the DCE-pMRI data set and the derived AIF, quantitative perfusion parameter (PBF, PBV, and MTT) maps can be calculated with the methods described e.g. by Ohno *et al.* [3].

## 3 Results and Discussion

In an ongoing study, 14 DCE-pMRI data sets from 7 adult male patients were acquired. Six of them suffer from COPD of different severity and one patient suffers from mild asthma. For each patient we had data sets from two scans with about 24 hours in between to investigate the repeatability. For all data sets the presented method correctly identified the branching point within the pulmonary artery. The results for two patients (baseline and follow-up examinations) are shown in Figure 2. While for one patient (A,B) only the pulmonary artery and the right ventricle remain after the image processing steps which are described above, in the other patient (C,D) connected parts of the CA-delivering vein are still present. This is due to the fact that this vein passes by the right pulmonary artery very closely and cannot be separated by the performed connected components analysis. However, for the presented

purpose this is sufficient because the graph analysis step correctly detects the branching point from the skeleton in all cases. For other purposes, e.g. an exact segmentation of the pulmonary artery, the method needs to be further refined. However, the output of the presented method can provide valuable input, like appropriate starting points, for segmentation algorithms. Size and shape of the ROI which includes the voxels which are considered for the AIF curve are assumed to be fixed (circular, 32 voxels) in the current implementation. A study which investigates if this is an appropriate assumption is subject to future work. Strong motion artefacts which we did not encounter in our pool of data sets might require a motion correction step prior to the proposed calculations.

The computation time for the automatic AIF detection is in the range of few seconds on a standard PC. This time is almost negligible as the method works fully automatic and the computations can be performed as a processing step during data import.

## 4 Conclusions

The presented work eliminates the influence of a person who draws the AIF manually on the outcome of quantitative pulmonary perfusion analysis. Hence, a better comparability of longitudinal perfusion examinations and examinations of different patients is potentially enabled which has to be investigated in a further study together with clinical partners. The automation of the AIF determination allows to generate the perfusion parameter maps in a preprocessing step already during data import. As a result the maps are available and can be analyzed as soon as the data set is examined.

## Acknowledgements

The work was supported by the Competence Network Asthma/COPD ([www.asconet.net](http://www.asconet.net)) funded by the German Federal Ministry of Education and Research (FKZ 01GI0881-0888). Patient data is courtesy of University Hospital Heidelberg and University Hospital Mainz.

## References

- [1] J. Biederer. General requirements of MRI of the lung and suggested standard protocol. In H. U. Kauczor, editor, *MRI of the lung*, pages 3–16. Springer, Berlin Heidelberg, 2009.
- [2] K. Mouridsen, S. Christensen, L. Gyldensted, and L. Østergaard. Automatic selection of arterial input function using cluster analysis. *Magnetic Resonance in Medicine*, 55(3):524–531, 2006.
- [3] Y. Ohno, H. Hatabu, K. Murase, T. Higashino, H. Kawamitsu, H. Watanabe, D. Takenaka, M. Fujii, and K. Sugimura. Quantitative assessment of regional pulmonary perfusion in the entire lung using three-dimensional ultrafast dynamic contrast-enhanced magnetic resonance imaging: Preliminary experience in 40 subjects. *Journal of Magnetic Resonance Imaging*, 20(3):353–365, 2004.
- [4] F. Risse. MR perfusion in the lung. In H. U. Kauczor, editor, *MRI of the lung*, pages 25–34. Springer, Berlin Heidelberg, 2009.
- [5] L. Østergaard, R. M. Weisskoff, D. A. Chesler, C. Gyldensted, and B. R. Rosen. High resolution measurement of cerebral blood flow using intravascular tracer bolus passages. Part I: Mathematical approach and statistical analysis. *Magnetic Resonance in Medicine*, 36(5):715–725, 1996.